RESEARCH ARTICLE

# A *TRP1*-marker-based system for gene complementation, overexpression, reporter gene expression and gene modification in *Candida glabrata*

Marcel Sprenger[1], Sascha Brunke[1], Bernhard Hube[1,2] and Lydia Kasper[1,*,†]

[1]Department Microbial Pathogenicity Mechanisms, Leibniz Institute for Natural Product Research and Infection Biology, Hans Knoell Institute, Adolf-Reichwein-Straße 23, 07745 Jena, Germany and [2]Institute of Microbiology, Friedrich Schiller University, Neugasse 25, 07743 Jena, Germany

*Corresponding author: Department Microbial Pathogenicity Mechanisms, Leibniz Institute for Natural Product Research and Infection Biology, Hans Knoell Institute, Adolf-Reichwein-Straße 23, 07745 Jena, Germany. Tel: +49 3641 5321219; E-mail: lydia.kasper@leibniz-hki.de

**One sentence summary:** Introduction of a gene complementation and reporter gene expression strategy for the human-pathogenic yeast *Candida glabrata*, based on genomic integration at the *TRP1* locus.

## ABSTRACT

Although less prevalent than its relative *Candida albicans*, the yeast *Candida glabrata* is a successful pathogen of humans, which causes life-threatening candidiasis. It is thus vital to understand the pathogenicity mechanisms and contributing genes in *C. glabrata*. However, gene complementation as a tool for restoring the function of a previously deleted gene is not standardized in *C. glabrata*, and it is less frequently used than in *C. albicans*.

In this study, we established a gene complementation strategy using genomic integration at the *TRP1* locus. We prove that our approach can not only be used for integration of complementation cassettes, but also for overexpression of markers like fluorescent proteins and the antigen ovalbumin, or of potential pathogenicity-related factors like the biotin transporter gene *VHT1*. With urea amidolyase Dur1,2 as an example, we demonstrate the application of the gene complementation approach for the expression of sequence-modified genes. With this approach, we found that a lysine-to-arginine mutation in the biotinylation motif of Dur1,2 impairs urea-dependent growth of *C. glabrata* and *C. albicans*. Taken together, the *TRP1*-based gene complementation approach is a valuable tool for investigating novel gene functions and for elucidating their role in the pathobiology of *C. glabrata*.

**Keywords:** *Candida glabrata*; *TRP1*; gene complementation; overexpression; green fluorescent protein; ovalbumin; urea amidolyase

## INTRODUCTION

The opportunistic pathogen *Candida glabrata* is a haploid fungus, which belongs to the Nakaseomyces clade (Kurtzman and Robnett 2003) and is closely related to the baker's yeast *Saccharomyces cerevisiae* (Bolotin-Fukuhara and Fairhead 2014; Gabaldón and Carrete 2016). *Candida glabrata* is normally associated with a mammalian host and is the second most prevalent *Candida* species to cause life-threatening candidiasis, after *Candida albicans* (Diekema *et al.* 2012; Galocha *et al.* 2019). It

is therefore necessary to understand and characterize mechanisms and genes contributing to the pathogenicity of this fungus.

The molecular Koch's postulates define criteria that must be satisfied to prove the contribution of a certain gene to pathogenesis (Falkow 1988). One of these criteria states that reintegration of the original gene into a mutated organism (complementation) should restore its pathogenic potential. Thus, complementation is an important step in elucidating gene functions and to exclude potential pleiotropic effects that originate from genetic manipulation. However, to date, gene complementation strategies in *C. glabrata* are less well developed than e.g. in *C. albicans*, less frequently used, and each have certain disadvantages. The first strategy used for *C. glabrata* is based on episomal replicative vectors (Kitada, Yamaguchi and Arisawa 1996; Frieman, McCaffery and Cormack 2002; Zordan *et al.* 2013), which contain autonomously replicating sequences (ARS) and a centromere (CEN) together with the gene of interest (GOI). An example is the centromere-based plasmid pCgACT which contains the nutritional marker *TRP1* to restore prototrophy of a *trp1*Δ deletion mutant (Miyazaki *et al.* 2011; Hosogaya *et al.* 2013; Noble *et al.* 2013). A strong disadvantage of episomal vectors is, however, unpredictable multimerizations or recombinations with the genome, causing unwanted genetic alterations (Pla *et al.* 1996). Additionally, plasmid loss (for example, in non-selective environments where tryptophan is readily available) or copy number variations could increase population heterogeneity (Zordan *et al.* 2013).

A second strategy for the generation of *C. glabrata* complementation strains relies on genomic integration, either by re-introducing the original gene of interest (GOI) together with specific selection markers at its native locus (Yánez-Carrillo *et al.* 2015), or by replacing the *URA3* gene by the GOI and the dominant *NAT1* marker (Nevitt and Thiele 2011). Both strategies have the potential to restore the gene of interest to a wild type-like state. The *NAT1* selection marker is, however, widely used for gene deletions in *C. glabrata* (Schwarzmüller *et al.* 2014) and therefore often not available anymore for later gene complementation. In addition, changes in *URA3* expression levels, depending on the gene locus, might influence virulence phenotypes (Brand *et al.* 2004).

Gene complementation in the diploid yeast *C. albicans* often uses the CIp10 strategy (Murad *et al.* 2000), whereby the selection marker *URA3* is ectopically expressed at one of the alleles of the neutral *RPS1* locus. In contrast to *C. albicans*, the haploid genome of *C. glabrata* makes it more difficult to find suitable loci, since single-allele knock-outs and dosage effects of ectopic expression of nutritional selection markers cannot be compensated by a second allele, with unknown influences on the phenotype.

In this study, we describe a novel gene complementation strategy for *C. glabrata* based on transformation with and stable genomic integration of a complementation cassette into the *TRP1* (CAGL0C04092g) locus. We show that re-integration of *TRP1* at this native chromosomal location can restore tryptophan prototrophy to wild type-like levels. This strategy can not only be used for gene complementation but also for reporter gene expression, gene overexpression, heterologous expression and expression of genetically modified gene variants in the haploid yeast *C. glabrata*.

We validate the functionality of our complementation system by heterologous expression of fluorescence reporter genes and of ovalbumin (OVA). Artificial OVA expression by pathogens is frequently used as a tool to investigate the cross-reactivity between effector and memory T cells in response to the microbe

(Ishizuka *et al.* 2009; Krummey *et al.* 2014; Harms *et al.* 2018). Further, we use the complementation system to overexpress the *C. glabrata* biotin importer gene *VHT1* (Sprenger *et al.* 2020) and to introduce point mutations into the biotinylation motif of the urea amidolyase gene *DUR1,2* (Roon and Levenberg 1972; Navarathna *et al.* 2012).

## RESULTS AND DISCUSSION

### Complementation of tryptophan auxotrophy in *C. glabrata* by genomic re-integration

Gene complementation in the best-studied *Candida* species, *C. albicans*, is often achieved by genomic integration into coding genes like *ADH1* (Hünniger *et al.* 2014), *RPS1* (Murad *et al.* 2000), or *ACT1* (Morschhäuser, Michel and Hacker 1998; Vandeputte *et al.* 2011; Xu *et al.* 2014). Integration in these loci disrupts one allele of the target gene in the diploid *C. albicans* genome which, in most cases, does not significantly affect growth or fitness of transformants.

In contrast, similar approaches in the haploid genome of *C. glabrata* lead to a complete knock-out of the original gene at the target locus. For selection of a target gene for complementation in *C. glabrata*, we therefore relied on previously published data. We chose the tryptophan biosynthesis gene *TRP1* (CAGL0C04092g), as genetic manipulation in this locus or even complete lack of *TRP1* did not impair *C. glabrata* survival in a systemic *C. glabrata* infection model (Jacobsen *et al.* 2010) or in macrophages (Schwarzmüller *et al.* 2014; Seider *et al.* 2014). In addition, the *TRP1* gene is, in addition to *HIS3*, *LEU2* and *URA3*, widely used as selection marker for different plasmid vectors in *S. cerevisiae* and *C. glabrata*.

As a basis for complementation constructs, we created a pTRP1 plasmid vector based on the plasmid pUC19 (Norrander, Kempe and Messing 1983). This new plasmid harbors the *TRP1* gene as the selection marker together with its up- and downstream regions for homologous recombination at the native *TRP1* locus (Sprenger *et al.* 2020). A multiple cloning site remains downstream of the *TRP1* terminator to allow easy insertion of any GOI (Fig. 1A). A *trp1*Δ mutant, which can be used as the parental strain for integration of pTRP1, has been previously created using the *SAT1* flipper protocol (Jacobsen *et al.* 2010). In this strain only a single recombination site (FRT) and no selection marker remain at the *TRP1* locus (Fig. 1B).

We started by generating a *TRP1* complementation strain from this strain. The *TRP1* construct was PCR-amplified from pTRP1 and used to transform *trp1*Δ, replacing the FRT sequence in the original *TRP1* locus. We used a PCR-amplified complementation cassette instead of the whole plasmid to rule out any unspecific genomic integration of additional vector DNA. Correct integration into the *TRP1* locus was then verified by Southern blotting (Fig. 1C). Phenotypically, the growth of the complemented strain (*trp1*Δ + *TRP1*) was fully restored in minimal medium lacking tryptophan (Fig. 1D). Based on these data, we conclude that the *TRP1* locus is suitable for expression of target genes. Our approach is therefore similar to the CIp10 strategy in *C. albicans* (Murad *et al.* 2000), but uses the native chromosomal location of the *TRP1* locus.

To apply our approach for the analysis of gene functions, a mutant strain lacking the GOI has to be generated in a *trp1*Δ strain background. This mutant will then be transformed with the *TRP1* cassette with or without the GOI, to restore *TRP1* prototrophy or create a *TRP1*-isogenic complemented strain.
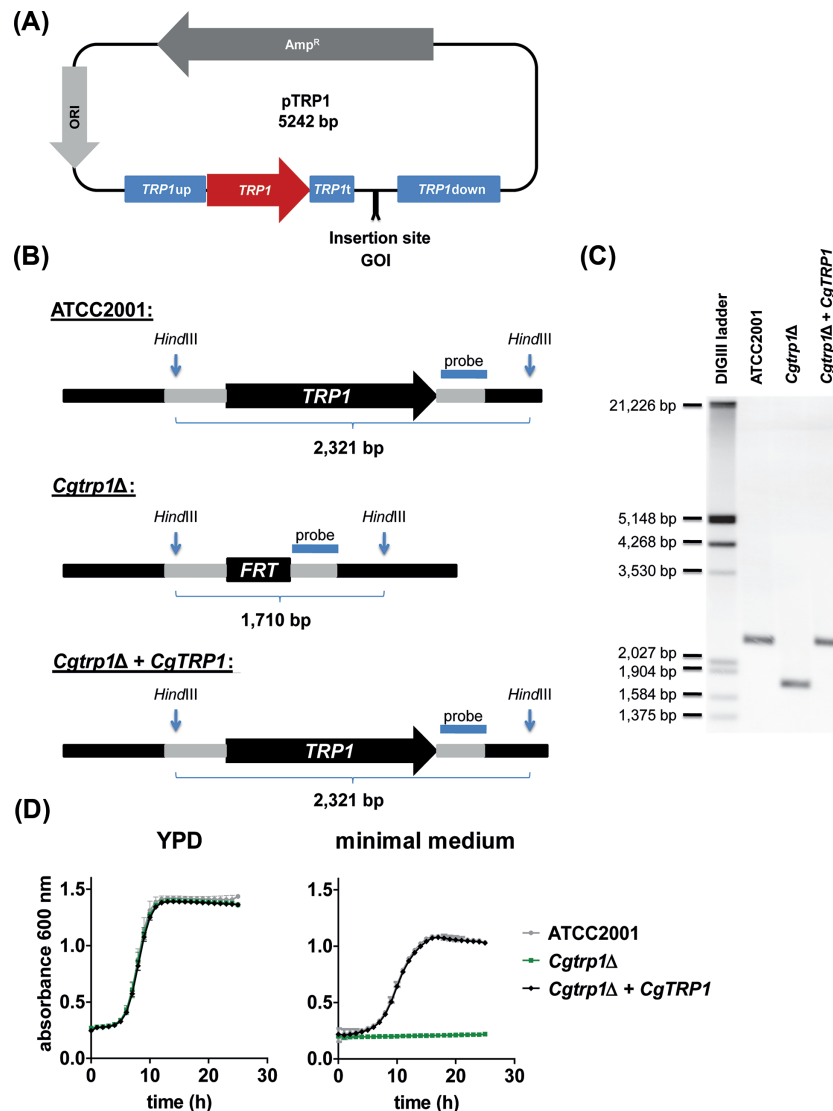
**Figure 1. Construction and verification of *TRP1* complemented strains. (A)**, Overview of the pTRP1 plasmid used for gene complementation in *C. glabrata*. The insertion site allows cloning of gene of interest (GOI) sequences with promotor and terminator regions. **(B)**, Depiction of the *TRP1* gene locus in the *C. glabrata* ATCC2001 reference genome, the *trp1* deletion mutant (*Cgtrp1Δ*) and our complementation strain (*Cgtrp1Δ + CgTRP1*). A DNA probe was designed for the terminator region to detect gene-specific fragments by Southern blotting. **(C)**, Southern blot of *Hind*III-digested genomic DNA of ATCC2001, *Cgtrp1Δ*, and *Cgtrp1Δ + CgTRP1* (*Cg* wt). The expected sizes from (b) correspond to the visible bands. **(D)**, Growth analysis of *C. glabrata* ATCC2001, *Cgtrp1Δ* and *Cgtrp1Δ + CgTRP1* in nutrient-rich medium (YPD) and minimal medium (SD) at 37°C for 24 h. Values are absorbance at 600 nm and are shown as mean ± SD of at least three replicates.

This method then allows the direct comparison of three prototrophic strains—the *trp1Δ + TRP1* wild type-like strain (Fig. 1), the *trp1ΔGOIΔ + TRP1* mutant strain and the *trp1ΔGOIΔ + TRP1 + GOI* complemented strain. We have successfully applied this strategy for complementation of *C. glabrata* mutants with the biotin metabolism genes *VHR1* and *VHT1*, for which recovery of wild type phenotypes after complementation was proven (Sprenger *et al.* 2020).

Gene complementation approaches help to verify the results of functional genomics approaches like large-scale screening of deletion mutant libraries (Janbon *et al.* 2019). Of note, our strategy of restoring the tryptophan prototrophy of a *TRP1*-deleted parental strain can be used to complement genes in a published triple auxotrophic *his3Δ leu2Δ trp1Δ C. glabrata* mutant library (Schwarzmüller *et al.* 2014). In this case, the leucine and histidine auxotrophies remain for further genetic manipulations. An alternative strategy to our *TRP1*-based method can be the integration of complementation cassettes into intergenic or promotor regions, which is already established in *C. albicans* (Davis *et al.* 2002; Staab, Bahn and Sundstrom 2003; Gerami-Nejad *et al.* 2013) and in *C. glabrata* (Ueno *et al.* 2011). However, genomic integration in these regions can raise the problem of inefficient transcriptional activity due to a silenced chromatin structure (Rando and Winston 2012; Gartenberg and Smith 2016).

## Heterologous expression of yEGFP, mCherry, and ovalbumin in *C. glabrata*

We next determined whether the *TRP1* locus is suitable for heterologous expression of markers like fluorescent proteins or ovalbumin, an antigen often used in immunological studies. We used the In-Fusion HD cloning system to fuse different promotors with these GOIs and into the *Xba*I-digested pTRP1 vector (Fig. 2A). This technique allows the combination of promotor, protein-encoding, and terminator sequences in a single cloning step.

Three well-investigated promotors (Zordan *et al.* 2013) were each fused to the gene encoding yEGFP (yeast-enhanced green
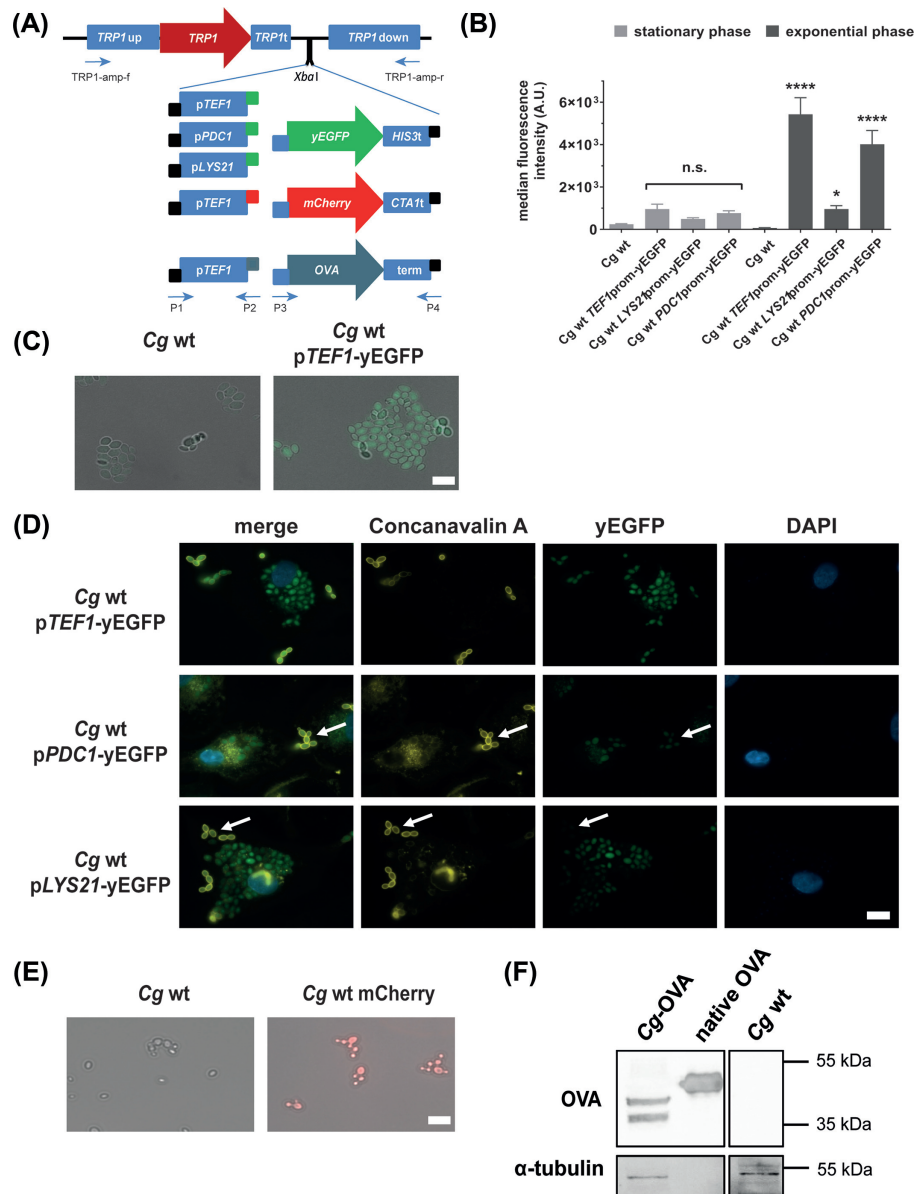
**Figure 2. Heterologous expression of yEGFP, mCherry, and ovalbumin in *C. glabrata*. (A)**, Overview of constructed plasmids for yEGFP, mCherry, and ovalbumin (OVA) expression in *C. glabrata*. Three different promotors were PCR-amplified and combined with PCR-amplified yEGFP. Similarly, the constitutive *CgTEF1* promotor was combined with PCR-amplified mCherry or OVA. Narrow bars: Amplification primers introduced ≥15 bp overlaps to the pTRP1 plasmid (black), promotor (blue) or yEGFP/mCherry/OVA (green/red/grey). Promotor and coding sequences were fused and cloned into an *XbaI*-linearized pTRP1 plasmid *via* the InFusion Cloning system. Primers used for PCR amplification are indicated. **(B)**, Flow cytometric analysis of median fluorescence intensity in arbitrary units (A.U.). Cells grown in YPD at 37°C and 180 rpm (stationary phase) were diluted 1:20 in fresh YPD and incubated 2 h under the same growth conditions (exponential phase). Yeast cells of both growth phases were analyzed for green fluorescence (FITC channel) using the BD FACS Verse. Values are shown as mean ± SD of four replicates. For statistical analysis, a repeated measures ANOVA with Bonferroni's multiple comparison test was performed, comparing fluorescent strains to wt (*$P \leq 0.05$, ***$P \leq 0.001$, ****$P \leq 0.0001$). **(C)**, Representative fluorescence microscopy image of stationary phase yeast cells grown in minimal medium. **(D)**, Representative fluorescence microscopy image of primary human macrophages (MDMs) after infection with yeast cells (MOI 5) for 3 h at 37°C and 5% $CO_2$. Non-phagocytosed yeast cells were counterstained with Alexa Fluor 647-coupled concanavalin A (representative examples shown by arrows). **(E)**, Representative fluorescence microscopy image of stationary phase yeast cells containing mCherry grown in minimal medium. Scale bar (C-E): 10 μm. **(F)**, Representative Western Blot image of OVA expression. Equal amounts of protein extracts of the OVA-expressing *C. glabrata* (*Cg*-OVA), the isogenic strain (*Cg* wt) and isolated egg white ovalbumin (OVA) were blotted and probed for OVA. A separate blot with the same amounts was probed for α-tubulin (loading control). Uncropped images are shown in Fig. S1.

fluorescent protein (Cormack *et al.* 1997)). The promotors were selected to achieve constitutive expression under *in vitro* conditions (*TEF1* and *PDC1* promotors), but also induced expression upon phagocytosis by macrophages (*LYS21* promotor). The correct integration into the *TRP1* locus of the *trp1Δ* strain was verified by PCR, and positive clones were analyzed for yEGFP fluorescence by microscopy and FACS.

As expected from a previous study (Zordan *et al.* 2013), we observed differences in fluorescence levels depending on the strength of the promotor and promotor-specific induction conditions: Expression of yEGFP under control of the *TEF1* promotor led to the highest median fluorescence intensity among all tested promotors in culture medium (Fig. 2B and C). Fluorescence was strongly induced in exponentially growing cells

compared to stationary cells (Fig. 2B). The *TEF1* promotor-controlled construct was furthermore highly expressed by *C. glabrata* cells internalized by macrophages, but also by non-internalized cells (Fig. 2D). *Candida glabrata* cells containing the *PDC1* promotor-controlled yEGFP expression construct showed fluorescence levels similar to cells containing the *TEF1* promotor construct in culture medium (Fig. 2B). Fluorescence was detected in macrophage-internalized and in non-internalized *C. glabrata* cells (Fig. 2D). When yEGFP expression was controlled by the *LYS21* promotor, the fluorescence signal was higher in macrophage-internalized than in extracellular *C. glabrata* cells (Fig. 2D, as expected from a previous study (Zordan *et al.* 2013)). In contrast to the other promotors, the expression of yEGFP remained low in the exponential growth phase when controlled by the *LYS21* promotor (Fig. 2B).

To further validate the usefulness of the strategy, the proven strong constitutive *TEF1* promotor was fused with mCherry (red fluorescent protein), cloned into the *Xba*I-digested pTRP1, and used to transform the *trp1Δ* strain. The expression of mCherry controlled by the *TEF1* promotor led to a strong fluorescence signal in the stationary phase (Fig. 2E).

With this, we provide a set of plasmids for fluorescence reporter-based analysis that integrate into the *TRP1* locus of *C. glabrata*. The expression of fluorescent markers under control of constitutive or inducible promotors is not only useful for generating fluorescently labeled fungal wild type or mutant strains that can be traced during infection. It also generates reporter strains that can be used to identify conditions that induce the respective promotors during infection (Miramón *et al.* 2012). In addition, the efficiency of transcription from promotors of interest can be quantified by measuring the fluorescence intensity even on a single cell level. This technique also opens up the possibility to distinguish *C. glabrata* strains with different fluorescent markers in combined infection or competition experiments.

The heterologous expression of ovalbumin (OVA) in pathogens is used as a tool to induce OVA-specific immune responses for investigation of the immune recognition of these pathogens and T cell activation (Ishizuka *et al.* 2009; Krummey *et al.* 2014; Harms *et al.* 2018). To generate an OVA-expressing *C. glabrata* strain, we fused an OVA gene version, which had been codon-optimized for *C. glabrata*, with the *TEF1* promotor and cloned it into the *Xba*I-digested pTRP1. Codon optimization was done to increase OVA expression in *C. glabrata*, as yeast and *Gallus gallus* have different codon usage frequencies (Branlant and Branlant 1985). The expression of OVA in *C. glabrata* was verified by Western blot (Fig. 2F). The heterologously expressed OVA in *C. glabrata* was smaller in size than native ovalbumin from egg white and was detected as two bands. A previous study in the yeast *Pichia pastoris* demonstrated that these two bands correspond to mono- and diglycosylated OVA. The smaller size of *C. glabrata*-expressed OVA is likely due to missing N-acetylation and phosphorylation in yeasts as opposed to chicken (Ito and Matsudomi 2005).

### Overexpression of the biotin transporter gene *VHT1* modulates intracellular survival within macrophages

To evaluate the suitability of our *TEF1*, *LYS21* and *PDC1* promotor constructs for overexpression of *C. glabrata*'s own genes, we used the system to overexpress the *C. glabrata* biotin transporter gene *VHT1*. *Candida glabrata* is auxotrophic for biotin and strictly relies on Vht1, the ortholog of an *S. cerevisiae* biotin importer, for biotin

uptake from the environment (Sprenger *et al.* 2020). The native promotor of *VHT1* is activated by the transcriptional regulator Vhr1 when biotin in the environment is limiting (Sprenger *et al.* 2020).

Similar constructs as described for yEGFP were created and used to transform a *trp1Δ* strain (wild type) and a *trp1Δ/vhr1Δ* strain (mutant). The resulting strains were analyzed for their *VHT1* transcript abundance in nutrient-rich medium—a condition in which *VHT1* expression from its native promotor is low (Sprenger *et al.* 2020). The transcript abundance of *VHT1* was strongly increased compared to the wild type when the gene was controlled by constitutive *TEF1* or *PDC1* promotors, whereas *LYS21*-controlled *VHT1* expression was only marginally increased (Fig. 3A). Overexpression of *VHT1* at the *TRP1* locus was independent of its native regulator, Vhr1, as the deletion of *VHR1* had no impact on the transcript abundance of *VHT1*.

A *vhr1Δ* mutant has reduced survival in macrophages (Sprenger *et al.* 2020). To test whether artificial up-regulation of its regulatory target *VHT1* can rescue this survival defect, we confronted monocyte-derived macrophages (MDMs) with *vhr1Δ* strains overexpressing *VHT1* and evaluated survival of phagocytosed fungal cells. As previously described, the *vhr1Δ* strain showed a lower intracellular survival than the wild type. In contrast, the *vhr1Δ* strains overexpressing *VHT1* reached higher survival rates, which were comparable to the wild type (Fig. 3B). These data imply that the overexpression of *VHT1* alone can indeed compensate the deletion of *VHR1*, whereas the wild type with its functional Vhr1 does not benefit from higher *VHT1* expression (Fig. 3B).

### Mutations in the biotinylation motif of Dur1,2 prevent the utilization of urea

Biotin is needed for central metabolic pathways, where it acts as a cofactor of biotin-dependent enzymes (Knowles 1989; Zempleni, Wijeratne and Hassan 2009; Tong 2013). Biotin is covalently linked to lysine residues of target proteins (Lane *et al.* 1964; Sternicki *et al.* 2017). Most of these lysine residues can be found in highly conserved AMKM sequence motifs of biotin-dependent enzymes (Samols *et al.* 1988; Chapman-Smith and Cronan 1999). The enzyme, urea amidolyase Dur1,2 possesses such a conserved biotinylation motif in the C-terminal carboxylase domain in both, *C. glabrata* and *C. albicans* (Fig. 4A, (Samols *et al.* 1988; Chapman-Smith and Cronan 1999)). Dur1,2 is important for using urea as a nitrogen source (Navarathna *et al.* 2011) and is necessary for the pathogenicity of *C. albicans* (Ghosh *et al.* 2009; Navarathna *et al.* 2012) and *C. glabrata* (Brunke *et al.* 2015). To study whether biotinylation is important for Dur1,2 function, we mutated the lysine codon AAA into the arginine-coding AGA (amino acid position 1798 in *C. glabrata* and 1779 in *C. albicans* (Fig. 4B)), using our newly developed complementation strategy in *C. glabrata* and the established CIp10-based strategy in *C. albicans*. As expected, *C. glabrata* and *C. albicans* deletion mutants lacking *DUR1,2* showed growth defects in liquid and solid media containing urea as the sole nitrogen source, while the wild type or a mutant strain with re-integration of one wild type copy of *DUR1,2* grew well (Fig. 4C–F). The mutants failed to grow in urea-containing liquid media and formed smaller colonies than the wild type on solid media (although some growth rescue seems to take place in close proximity to urea-metabolizing colonies, Fig 4F). The *C. albicans dur1,2Δ/Δ* mutant also failed to induce colony wrinkling at 37°C (Fig. 4F). Mutant strains with re-integration of *DUR1,2* carrying a K→R point mutation in the
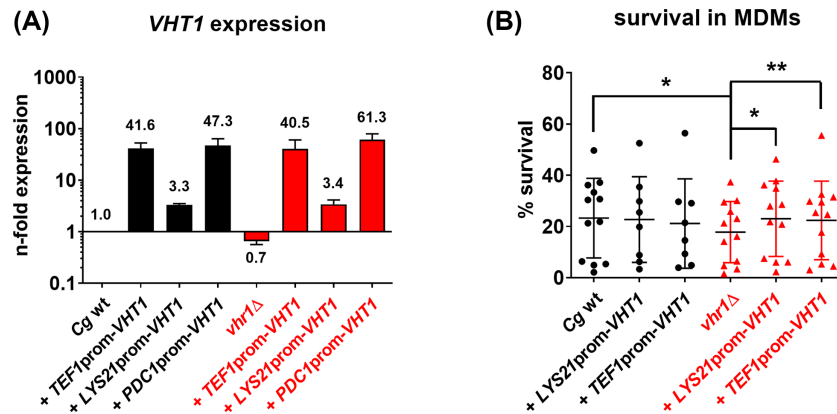
**Figure 3.** The overexpression of *CgVHT1* increases intracellular fitness of *Cgvhr1Δ*. **(A)**, *Candida glabrata* wt (black letters), mutant (*Cgvhr1Δ*, red letters) and corresponding overexpression strains (+*LYS21*prom-*VHT1*, +*TEF1*prom-*VHT1*, +*PDC1*prom-*VHT1*) were cultivated in YPD for 90 min at 37°C and 180 rpm. Target gene expression was analyzed by qRT-PCR and normalized to *ACT1* and *EFB1*. Expression is shown relative to the *Cg* wt strain. Data are shown as mean ± SD of two independent experiments. **(B)**, *Candida glabrata* wt (black letters), mutant (*vhr1Δ*, red letters), and corresponding overexpression strains (+p*LYS21*-*VHT1*, +p*TEF1*-*VHT1*) were pre-cultured in YPD + 2 mg/L biotin before confrontation with MDMs. Survival of *C. glabrata* strains after 3 h co-incubation with MDMs at an MOI of 1 is shown as survival in % of inoculum (mean ± SD). Each single dot represents one individual blood donor (in total at least two independent experiments with four donors each). For statistical analysis, a repeated measures ANOVA with Bonferroni's multiple comparison test was performed comparing all strains (*$P \leq 0.05$, **$P \leq 0.01$).

biotinylation motif phenocopied the *dur1,2* deletion mutants in both species (Fig. 4C–F). These data suggest that biotinylation of Dur1,2 is indeed essential for urea utilization in *C. glabrata* and *C. albicans*.

## MATERIALS AND METHODS

### Ethics statement

Human blood was taken from healthy volunteers with written, informed consent. The blood donation protocol and use of blood for this study were approved by the institutional ethics committee of the university hospital Jena (Ethik-Kommission des Universitätsklinikums Jena, Permission No. 2207–01/08).

### Strains and growth conditions

All strains used in this study are listed in Table 1. *Escherichia coli* was cultured in liquid lysogeny broth (LB) at 37°C with shaking at 180 rpm and with 50 µg mL$^{-1}$ ampicillin for plasmid propagation. *Candida* strains were cultured in liquid Yeast Peptone Dextrose (YPD) broth (2% glucose, 2% peptone, 1% yeast extract) at 30°C (*C. albicans*) or 37°C (*C. glabrata*), with shaking at 180 rpm for 14–16 h. For growth on solid medium, 2% agar was added. Routinely, stationary phase yeast cells from pre-cultures were washed three times in PBS, and the cell number was adjusted in PBS or culture medium.

For growth analyses in liquid media, 20 µL of a yeast cell suspension (5 × 10$^6$ cells mL$^{-1}$) were added to 180 µL media in a 96-well plate (Tissue Culture Test Plate, TPP Techno Plastic Products AG). In some experiments, minimal medium (0.19% yeast nitrogen base (YNB) without biotin, amino acids and ammonium sulfate [Formedium]; 2% glucose) with varying biotin concentrations and different nitrogen sources (0.5% ammonium sulfate, 0.5% urea) was used. Growth was monitored by measuring the absorbance at 600 nm every 30 min for 100 cycles at 30°C or 37°C using a microplate reader (Plate Reader infinite M200 PRO, Tecan Group GmbH) with orbital shaking (30 s, amplitude: 6 mm, wait: 10 s) before each measurement and multiple reads per well. All experiments were performed in technical duplicates and, at least, biological triplicates. Growth of *Candida* on solid agar was tested by spotting serial dilutions (1 × 10$^6$ to 1 × 10$^1$) of yeast cells

on YNB plates (0.19% YNB without amino acids and biotin; 2% glucose; either 0.5% ammonium sulfate or 0.5% urea; 2% oxoid agar).

### Construction of VHT1 overexpression, OVA overexpression and fluorescently labelled strains

Plasmids and primers used for strain construction are listed in Table 2 and Table S1 (Supporting Information), respectively. For generation of overexpression strains, promotor and coding sequence fragments were introduced into the pTRP1 plasmid (Sprenger *et al.* 2020) by In-Fusion HD cloning (Takara), generating overexpression plasmids pTRP1-*TEF1*prom-*yEGFP*, pTRP1-*PDC1*prom-*yEGFP*, pTRP1-*LYS21* prom-*yEGFP*, pTRP1-*TEF1*prom-*mCherry*, pTRP1-*TEF1*prom-*OVA*, pTRP1-*TEF1*prom-*VHT1*, pTRP1-*PDC1*prom-*VHT1* and pTRP1-*LYS21*prom-*VHT1* (Table 2). First, promotor sequences of *TEF1*, *LYS21* or *PDC1* were PCR-amplified from *C. glabrata* genomic DNA with P1 and P2 primers (Fig. 2A; Table S1, Supporting Information). P1 primers introduced ≥15 bp overlaps to the pTRP1 plasmid sequence, while P2 primers introduced overlaps to the respective coding sequences (see below). In a second PCR-reaction, coding sequences of *yEGFP*, mCherry, ovalbumin (OVA) or *VHT1* were amplified using P3 and P4 primers (Fig. 2A; Table S1, Supporting Information). pCN-PDC1-GFP (Zordan *et al.* 2013) served as a PCR template for *yEGFP*, pYC56 (Yánez-Carrillo *et al.* 2015) for mCherry, and *C. glabrata* genomic DNA for *VHT1*. For OVA, a codon-optimized version of chicken ovalbumin synthesized by GeneArt Gene Synthesis (Thermo Fisher Scientific) was used as a PCR template. The constructs contained native (*VHT1*) or foreign terminator sequences (*HIS3* terminator for *yEGFP*, *CTA1* terminator for mCherry, and *Ashbya gossypii TEF1* terminator for OVA). P3 primers introduced ≥15 bp overlaps to the respective promotor sequences (see above), and P4 primers generated overlaps to the pTRP1 plasmid sequence. Promotor and coding sequence fragments were combined and cloned with the help of the In-Fusion HD cloning system (Takara Bio) into *Xba*I-digested pTRP1. An exception was pTRP1-*PDC1*prom-*yEGFP*, for which promotor and coding sequence was directly amplified form plasmid pCN-PDC1-GFP, using P1 and P4 primers, and cloned into pTRP1. The resulting plasmids were confirmed by PCR and sequencing, using primers

**(A)**

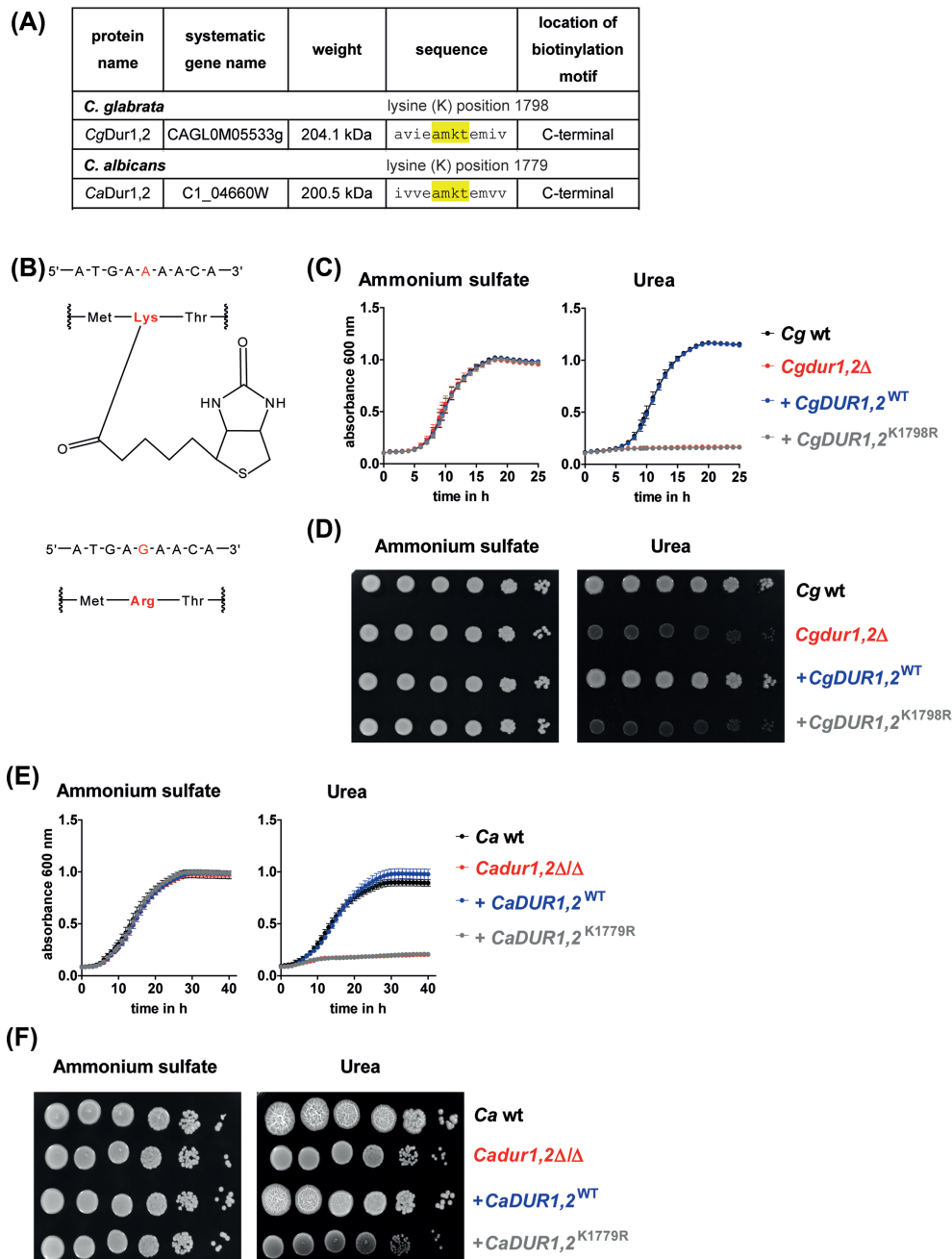| protein name | systematic gene name | weight | sequence | location of biotinylation motif |
|---|---|---|---|---|
| *C. glabrata* | | | lysine (K) position 1798 | |
| *Cg*Dur1,2 | CAGL0M05533g | 204.1 kDa | `avie`amkt`emiv` | C-terminal |
| *C. albicans* | | | lysine (K) position 1779 | |
| *Ca*Dur1,2 | C1_04660W | 200.5 kDa | `ivve`amkt`emvv` | C-terminal |



Figure 4. Biotinylation of Dur1,2 is essential for urea utilization. (A), Dur1,2 contains a highly conserved biotinylation motif (AMKT) in *C. glabrata* and *C. albicans*. (B), Upper part: DNA sequence, which is transcribed into the lysine (K) residue essential for biotinylation and biotin structure coupled to lysine. Lower part: The adenine of the triplet codon was mutated to guanine to induce an amino acid exchange to arginine. (C and D), Growth analysis of *C. glabrata* wt, *Cgdur1,2*Δ, +*CgDUR1,2*[WT], and + *CgDUR1,2*[K1798R] in liquid (c) or on solid (d) minimal medium at 37°C. (E, F), Growth analysis of *C. albicans* wt, *Cadur1,2*Δ/Δ, +*CaDUR1,2*[WT] and + *CaDUR1,2*[K1779R] in liquid (e, 30°C) or on solid (f, 37°C) minimal medium. Media contained either 0.5% ammonium sulfate or 0.5% urea as sole nitrogen source. Values are represented as mean ± SD of at least three replicates and representative pictures are shown.

listed in Table S1 (Supporting Information). The complete cassettes containing the *TRP1* selection marker together with the overexpression constructs were then PCR-amplified from pTRP1 overexpression plasmids using primers TRP1-amp-f and TRP1-amp-r (Table S1, Supporting Information; Fig. 2A). PCR products were purified and used to transform a tryptophan-auxotrophic *trp1*Δ strain (Jacobsen *et al.* 2010). The *VHT1* constructs were additionally transformed into a tryptophan-auxotrophic *vhr1*Δ strain (Sprenger *et al.* 2020). Transformation of *C. glabrata* strains was done using the modified heat-shock method ((Sangland

*et al.* 1996) with heat shock for 15 min at 45°C). Tryptophan-prototrophic clones with integration of the cassette into the native *TRP1* locus were selected after plating on solid minimal medium that lacks tryptophan. The correct integration into the *TRP1* locus was verified by PCR, and positive clones were analyzed for yEGFP and mCherry fluorescence by microscopy and FACS (only yEGFP).

In experiments that required comparisons to a wild type, the strain *Cgtrp1*Δ + *TRP1* was used as an isogenic wild type strain (*Cg* wt). This strain was generated by re-introducing *TRP1*,

**Table 1.** Strains used in this study.

| Strains | Internal ID | Designation/genotype | Reference |
|---|---|---|---|
| *C. glabrata* | | | |
| ATCC2001 | C94 | Clinical isolate | (Schwarzmüller *et al.* 2014) |
| *Cgtrp1Δ* | G17 | Parental strain (derivative of ATCC2001) *trp1::FRT* | (Jacobsen *et al.* 2010) |
| *Cgtrp1Δ + CgTRP1 (Cg* wt) | G203 | Isogenic wild type *trp1::TRP1* | (Sprenger *et al.* 2020) |
| *Cg* wt + OVA | G205 | *trp1::(TRP1-CgTEF1prom*(-1 to -1000)*-OVA)* | This study |
| *Cg* wt + *CgLYS21p-CgVHT1* | G247 | *trp1::(TRP1-CgLYS21prom*(-1 to -1157)*-CAGL0K04609g-CAGL0K04609g*term) | This study |
| *Cg* wt + *CgTEF1p-CgVHT1* | G249 | *trp1::(TRP1-CgTEF1prom*(-1 to -1000)*-CAGL0K04609g-CAGL0K04609g*term) | This study |
| *Cg* wt + *CgPDC1p-yEGFP* | G257 | *trp1::(TRP1-CgPDC1prom*(-1 to -973)*-yEGFP-CgHIS3*term) | This study |
| *Cg* wt + *CgLYS21p- yEGFP* | G259 | *trp1::(TRP1-CgLYS21prom*(-1 to -1157)*-yEGFP-CgHIS3*term) | This study |
| *Cg* wt + *CgTEF1p- yEGFP* | G261 | *trp1::(TRP1-CgTEF1prom*(-1 to -1000)*-yEGFP-CgHIS3*term) | This study |
| *Cg* wt + *CgTEF1p-mCherry* | G325 | *trp1::(TRP1-CgTEF1prom*(-1 to -1000)*-mCherry- CgCTA1*term) | This study |
| *Cgtrp1Δvhr1Δ* | G237 | *trp1::FRT CAGL0M12496g::NAT1* | This study |
| *Cgvhr1Δ* | G241 | *trp1::TRP1 CAGL0M12496g::NAT1* | (Sprenger *et al.* 2020) |
| *Cgvhr1Δ + CgLYS21p-CgVHT1* | G253 | *CAGL0M12496g::NAT1 trp1::(TRP1-CgLYS21prom*(-1 to -1157)*-CAGL0K04609g-CAGL0K04609g*term) | This study |
| *Cgvhr1Δ + CgTEF1p-CgVHT1* | G255 | *CAGL0M12496g::NAT1 trp1::(TRP1-CgTEF1prom*(-1 to -973)*-CAGL0K04609g-CAGL0K04609g*term) | This study |
| *Cgtrp1Δdur1,2Δ* | G330 | *trp1::FRT CAGL0M05533g::NAT1* | This study |
| *Cgdur1,2Δ* | G366 | *trp1::TRP1 CAGL0M05533g::NAT1* | This study |
| *Cgdur1,2Δ + CgDUR1,2* | G367 | *CAGL0M05533g::NAT1; trp1::(TRP1-CAGL0M05533g)* | This study |
| *Cgdur1,2Δ + CgDUR1,2*[K1798R] | G368 | *CAGL0M05533g::NAT1; trp1::(TRP1-CAGL0M05533g* with codon 1798: AAA → AGA) | This study |
| *C. albicans* | | | |
| BWP17 | M130 | Parental strain (derivative of SC5314) *ura3::λimm434/ura3::λimm434 his1::hisG/his1::hisG arg4::hisG/arg4::hisG* | (Wilson, Davis and Mitchell 1999) |
| BWP17 CIp30 (*Ca* wt) | M1477 | Isogenic wildtype *ura3::λimm434/ura3::λimm434 his1::hisG/his1::hisG arg4::hisG/arg4::hisG RPS1/rps1::CIp30-URA3-HIS1-ARG4* | (Citiulo *et al.* 2012) |
| *Caura3Δ/Δdur1,2Δ/Δ* | M2671 | *orf19.7468::ARG4/orf19.7468::HIS1* | This study |
| *Cadur1,2Δ/Δ* | M2672 | *orf19.7468::ARG4/orf19.7468::HIS1 RPS1/rps1::CIp10-URA3* | This study |
| *Cadur1,2Δ/Δ + CgDUR1,2* | M2674 | *orf19.7468::ARG4/orf19.7468::HIS1 RPS1/rps1::CIp10-URA3-orf19.7468* | This study |
| *Cadur1,2Δ/Δ + CgDUR1,2*[K1779R] | M2721 | *orf19.7468::ARG4/orf19.7468::HIS1 RPS1/rps1::CIp10-URA3-orf19.7468* with (codon 1779: AAA → AGA) | This study |
| *E. coli* | | | |
| Stellar™ Competent Cells | | *F–, endA1, supE44, thi-1, recA1, relA1, gyrA96, phoA, Φ80d lacZΔ M15, Δ (lacZYA-argF) U169, Δ (mrr—hsdRMS—mcrBC), mcrA, λ–* | In-Fusion® HD Cloning Plus Kit |

amplified from pTRP1 into the native *TRP1* locus into *Cgtrp1Δ* (Sprenger *et al.* 2020). The *Cgtrp1Δvhr1Δ* mutant strain carrying the *TRP1* complementation insert (*Cgvhr1Δ*; (Sprenger *et al.* 2020)) was constructed in a similar way.

### Construction of DUR1,2 deletion mutants

The *C. glabrata dur1,2Δ* mutant (CAGL0M05533gΔ) was generated in the *trp1Δ* parental strain. A deletion cassette was PCR-amplified from genomic DNA of a previously generated triple-auxotrophic *dur1,2Δ* mutant (Schwarzmüller *et al.* 2014) using primers CgDUR1,2amp fwd and rev (Table S1, Supporting Information)), followed by purification with the QIAquick® PCR purification kit (Qiagen). The transformation was performed as described above.

For interspecies comparison, a *C. albicans dur1,2Δ/Δ* (C1_04660WΔ/Δ) mutant was generated by a standard gene disruption method (Wilson, Davis and Mitchell 1999) using lithium

acetate transformation (Walther and Wendland 2003). Briefly, the Arg-, His-, and Ura-auxotrophic parental strain BWP17 was sequentially transformed with 10 µg of purified *HIS1* and *ARG4* deletion cassettes (amplified with primers CaDUR1,2 del fwd and rev from pFA-HIS1 and -ARG4 plasmids, respectively; Table 2 and Table S1, Supporting Information), which were flanked by 100 bp of the target homology region. Transformation resulted in disruption of the open reading frames of both alleles of C1_04660W, yielding strain *Caura3Δ/Δdur1,2Δ/Δ*. The correct deletion of *DUR1,2* in *C. glabrata* and *C. albicans* was confirmed by PCR and Southern blot.

### Construction of DUR1,2 complementation strains

*Candida glabrata DUR1,2* complementation strains were constructed as follows: The *DUR1,2* wild type allele together with its up- and downstream intergenic regions was PCR-amplified from *C. glabrata* genomic DNA with primers pTRP1-CgDUR1,2

**Table 2.** Plasmids used in this study.

| Plasmid | Used for | Reference |
|---|---|---|
| pFA-*HIS1* | Amplification of *CaHIS1* cassette | (Gola *et al.* 2003) |
| pFA-*ARG4* | Amplification of *CaARG4* cassette | (Gola *et al.* 2003) |
| CIp10 | Integration of *CaURA3* into *RPS1* locus | (Murad *et al.* 2000) |
| pTRP1 | Amplification of *CgTRP1* cassette, Basis for *TRP1* complementation constructs | (Sprenger *et al.* 2020) |
| pCN-PDC1-GFP | CEN/ARS episomal plasmid for *yEGFP* expression in *C. glabrata* under control of the *PDC1* promotor | (Zordan *et al.* 2013) |
| pYC56 | Recipient integrative vector harboring *mCherry* | (Yánez-Carrillo *et al.* 2015) |
| pTRP1-*LYS21*prom-*yEGFP* | Amplification of *CgTRP1* and *yEGFP* under control of the *LYS21* promotor | This study |
| pTRP1-*LYS21*prom-*VHT1* | Amplification of *CgTRP1* and CAGL0K04609g under control of the *LYS21* promotor | This study |
| pTRP1-*PDC1*prom-*yEGFP* | Amplification of *CgTRP1* and *yEGFP* under control of the *PDC1* promotor | This study |
| pTRP1-*PDC1*prom-*VHT1* | Amplification of *CgTRP1* and CAGL0K04609g under control of the *PDC1* promotor | This study |
| pTRP1-*TEF1*prom-*yEGFP* | Amplification of *CgTRP1* and *yEGFP* under control of the *TEF1* promotor | This study |
| pTRP1-*TEF1*prom-*VHT1* | Amplification of *CgTRP1* and CAGL0K04609g under control of the *TEF1* promotor | This study |
| pTRP1-*TEF1*prom-*OVA* | Amplification of *CgTRP1* and *OVA* under control of the *TEF1* promotor | This study |
| pTRP1-*TEF1*prom-*mCherry* | Amplification of *CgTRP1* and *mCherry* under control of the *TEF1* promotor | This study |
| CIp10-*CaDUR1,2* | Integration of *CaURA3* and *CaDUR1,2* (orf19.780) into *RPS1* locus | This study |
| CIp10-*CaDUR1,2* (K1779R) | Integration of *CaURA3* and orf19.780 (lysine 1779 mutated to arginine) into *RPS1* locus | This study |
| pTRP1-*CgDUR1,2* | Amplification of *CgTRP1* and *CgDUR1,2* (CAGL0M05533g) | This study |
| pTRP1-*CgDUR1,2* (K1798R) | Amplification of *CgTRP1* and CAGL0M05533g (lysine 1798 mutated to arginine) | This study |

fwd (P1) and pTRP1-CgDUR1,2 rev new (P4) that introduced ≥15 bp overlaps to the pTRP1 sequence (Table S1). The mutated version *DUR1,2*[K1798R] was created by combining P1 and P4 (see above) with internal primers P2 and P3, which introduce a single nucleotide change resulting in a codon exchange from lysine to arginine. The primer combinations P1 + P2 and P3 + P4 generated two PCR fragments with ≥15 bp overlaps to each other and to pTRP1. The wild-type allele (one fragment) or the mutated allele (two fragments) were cloned into *Xba*I-digested pTRP1 by In-Fusion HD cloning, generating plasmids pTRP1-*DUR1,2* and pTRP1-*DUR1,2* (K1798R), which were verified by sequencing. Cassettes containing only *TRP1* or *TRP1-DUR1,2*[WT] and *TRP1-DUR1,2*[K1798R] were then amplified from the complementation plasmids by PCR, purified, and used to transform a *Cgtrp1∆/dur1,2∆* mutant background strain to generate tryptophan prototrophic mutants and complemented strains with the native or mutated biotinylation motif, respectively. Resulting clones were selected for on solid minimal medium lacking tryptophan.

To generate *C. albicans DUR1,2* complementation strains, the coding sequence of *DUR1,2* was PCR-amplified together with the native up- and downstream intergenic regions from *C. albicans* genomic DNA with primers pCIp10-CaDUR1,2 fwd (P1) and pCIp10-CaDUR1,2 rev (P4) that introduced ≥15 bp overlaps to the pCIp10 sequence (Table S1). The mutated version *DUR1,2*[K1779R] was created using additional internal primers P2 and P3, as described above for *C. glabrata*. The wild type allele (one fragment) or the mutated allele (two fragments) were cloned by In-Fusion HD cloning into the CIp10 plasmid using *Xho*I, generating plasmids CIp10-*DUR1,2* or CIp10-*DUR1,2* (K1779R) (Table 2).

Constructed plasmids were verified by sequencing. Homozygous uridine-auxotrophic deletion mutants (*Caura3∆/∆dur1,2∆/∆*) were transformed with the *Stu*I-linearized empty CIp10 plasmid (Murad *et al.* 2000) to generate prototrophic mutants, or with *Stu*I-linearized CIp10-*DUR1,2* or CIp10-*DUR1,2* (K1779R) plasmids to generate complemented strains with the native or mutated biotinylation motif. Resulting clones were selected for on solid minimal medium lacking uridine.

The correct integration of *C. glabrata* and *C. albicans* complementation cassettes was confirmed by PCR and Southern blot.

## Genomic DNA isolation and Southern blot

Genomic DNA was isolated as described in (Millon *et al.* 1994). Briefly, cells form overnight cultures were protoplasted in lysis buffer (1 M sorbitol; 100 mM sodium citrate, pH 5.8; 50 mM EDTA, pH 8.0; 0.6 mg mL$^{-1}$ lyticase and 2.5% $\beta$-mercaptoethanol) at 37°C for 45 min. Protoplasts were then pelleted, resuspended in proteinase buffer (10 mM Tris-HCl, pH 7.5; 50 mM EDTA, pH 7.5; 0.5% SDS; 1 mg mL$^{-1}$ proteinase K) and incubated at 60°C for 30 min. After addition of phenol/chloroform/isoamylalcohol (25:24:1), vortexing for 4 min and centrifugation (20 000*g*, 5 min, RT), the aqueous phase was collected, and DNA was precipitated using isopropanol, washed with 70% ethanol and reconstituted in ddH$_2$O containing 10 mg mL$^{-1}$ RNase A. The DNA quantity was evaluated using a NanoDrop Spectrophotometer (ND-100, Peqlab). *Hind*III (NEB)-digested genomic DNA (30 µg) and the DNA Molecular Weight Marker III, DIG-labelled (50 pg; Roche) was separated by agarose gel electrophoresis. The DNA was depurinated with 0.25 M HCl and denatured with 0.5 M NaOH, 1.5 M NaCl.

The gel was neutralized with 1 M Tris-HCl pH 7.5; 1.5 M NaCl and equilibrated for at least 10 min in 20 × SSC (3 M NaCl, 0.3 M sodium citrate; pH 7.0).

The DNA was vacuum blotted 1.5 h at 50–100 mbar (Biometra) onto activated nylon membrane (positively charged, Roche). Following, the membrane was rinsed 30 sec in 0.4 M NaOH, 30 sec in 0.2 M Tris-HCl pH 7.5 and dried 10–15 min on a piece of Whatman™ filter paper. The DNA was crosslinked to the membrane by UV light (120 mJ/cm$^2$) for at least 60 sec and then rinsed with 2 × SSC. Further steps were performed according the DIG nonradioactive nucleic acid labeling and detection system (Roche), using the PCR DIG Probe Synthesis Kit, DIG Easy Hyb™, Anti-Digoxigenin-AP, Fab fragments, and CDP-Star.

## Fungal RNA isolation and quantitative reverse transcription PCR (qRT-PCR)

For preparation of RNA from *in vitro* cultures of *Candida*, stationary phase yeast cells were washed three times in PBS, and $2 \times 10^7$ *Candida* cells per mL were inoculated into minimal medium with different biotin concentrations. At indicated time points, cells were harvested and centrifuged (4000 × *g*, 10 min and 4°C). The cell pellet was washed with ice cold water, centrifuged again and immediately frozen in liquid nitrogen. The isolation of the fungal RNA was performed as previously described (Lüttich, Brunke and Hube 2012). The quantity of the RNA was determined using the NanoDrop Spectrophotometer ND-1000 (NRW International GmbH). DNase-treated RNA (600 ng) was transcribed into cDNA using 0.5 μg oligo-dT$_{12–18}$, 100 U Superscript™ III Reverse Transcriptase, and 20 U RNaseOUT™ Recombinant RNase Inhibitor (all: Thermo Fischer Scientific) in a total volume of 35 μL for 2 h at 42°C, followed by heat-inactivation for 15 min at 70°C. The cDNA was diluted 1:20 in DEPC-treated water and used for quantitative PCR with EvaGreen® QPCR Mix II (Bio&SELL) performed in a CFX96 thermocycler (Bio-Rad). Primers (Table S1, Supporting Information) were used at a final concentration of 500 nM. Target gene expression was calculated using the $\Delta\Delta Ct$ method (Pfaffl 2001), with normalization to the housekeeping genes *ACT1* and *EFB1*.

## Protein isolation and Western blot

For preparation of whole protein extracts, stationary phase cells were washed three times in PBS, diluted to OD$_{600}$ 0.2 into minimal medium and incubated at 37°C at 180 rpm overnight. The cells were harvested and mechanically lysed in PBS-KMT (PBS + 3 mM KCl, 2.5 mM MgCl$_2$, 0.1% Triton-X-100) with a protease inhibitor cocktail (Roche) using bead beating with acid-washed glass beads in a Precellys 24 homogenizer (Peqlab; 6500 rpm, 2 cycles, each 30 s, 15 s pause). The lysate was centrifuged (14 000 rpm, 4°C for 5 min) and the protein concentration of the supernatant was determined by Pierce™ BCA Protein Assay Kit (Thermo Fisher Scientific). Two aliquots of 20 μg protein of each sample were denatured in one-fourth volume of 4 × Lämmli buffer (125 mM Tris-HCl pH 6.8, 50% glycerol, 4% SDS, 0.02% bromophenol blue, 10% $\beta$-mercaptoethanol) at 95°C for 5 min and separated by denaturizing SDS-PAGE with Rotiphorese® Gel 30 (final 12% acrylamide mix (Roth)). Proteins were electro-transferred to nitrocellulose membranes (Whatman) in blotting buffer (25 mM Tris, 192 mM glycine, 10% methanol and 0.1% SDS) and free binding sites were blocked with 5% milk powder in TBS (0.5 M Tris, 1.5 M NaCl, pH 7.6) + 0.05% Tween®-20 (TBS-T) for 3 h at room temperature. One membrane was incubated with monoclonal mouse anti-chicken egg albumin antibody (Sigma), diluted 1:2000 in TBS-T containing 2% milk powder. The other membrane was incubated with rat anti-$\alpha$-tubulin antibody (AbD Serotec), diluted 1:1000 in TBS-T containing 2% BSA. Both were incubated at 4°C overnight with gentle shaking. The membranes were rinsed three times in TBS-T, incubated with goat anti-mouse IgG-HRP (1:1000 in 2% milk powder) or goat anti-rat IgG-HRP (1:2000 in 2% BSA) (both Santa Cruz Biotech) to detect ovalbumin and $\alpha$-tubulin, respectively. Finally, the membranes were rinsed three times in TBS-T and two times in TBS, followed by chemiluminescence detection using Pierce™ ECL Plus Western Blotting Substrate (Thermo Fisher Scientific) according to the manufactures' instructions. Protein sizes were estimated using PageRuler Plus prestained (Fisher Scientific), which was visible on the blot membrane. Marker band positions were determined by overlaying marker and chemiluminescence images. Full size scans of Western blots are provided in Fig. S1 (Supporting Information).

## Experiments with human monocyte-derived macrophages (MDMs)

Primary macrophages were differentiated from CD14-positive monocytes originating from independent blood donors as previously described (Sprenger *et al.* 2020), seeded in 24-well plates ($2 \times 10^5$ MDMs/well) in RPMI with 50 ng mL$^{-1}$ M-CSF, and incubated overnight. Prior to macrophage infection, the medium was exchanged to serum- and biotin-free RPMI with L-glutamine (Thermo Fisher Scientific) to exclude biotin uptake by *Candida* prior to phagocytosis.

Fungal survival was determined as described previously (Sprenger *et al.* 2020). Briefly, macrophages were infected with *C. glabrata* at a multiplicity of infection (MOI) of 1 (one well per *Candida* strain and donor). After 3 h, non-internalized *Candida* cells were removed by washing with PBS. Intracellular yeast cells were then released by lysing the macrophages with 0.1% Triton-X-100, and lysates were plated on YPD agar plates in duplicate. In parallel, culture inocula were plated on YPD. Survival rates were then calculated based on CFU numbers in macrophages lysates relative to CFU numbers of initial inocula.

For fluorescence microscopy after macrophage phagocytosis, $1.5 \times 10^5$ MDMs/well were allowed to adhere onto coverslips in a 24-well plate overnight in RPMI containing 50 ng mL$^{-1}$ M-CSF and 10% FBS, and then infected with *C. glabrata* at an MOI of 2 for the indicated time points. Phagocytosis was synchronized on ice for 30 min followed by two washing steps with pre-warmed medium to remove unbound *Candida* cells.

## Fluorescence analysis by flow cytometry and microscopy

Stationary phase cells were diluted 1:20 into fresh YPD medium and incubated at 37°C for 2 h and 180 rpm. Then, cells were harvested and washed once with PBS, fixed with 500 μL Roti®-Histofix 4% for 20 min and washed again with PBS. The median fluorescence intensity (MFI) of *C. glabrata* yeast cells was evaluated with BD FACS Verse® (BD Biosciences, Franklin Lakes (USA)) counting 50 000 events with the same instrument settings. Data analysis was performed using the FlowJO™ 10.2 software (FlowJO LLC, Ashland (USA)). The gating strategy was based on blotting forward (FSC) and side scatter (SSC) to exclude cellular debris, followed by gating for single cells by using FSC-W and FSC-H.

The staining of phagocytosed yeast cells was adapted from (Kasper *et al.* 2018). Infected macrophages were fixed with Roti®-Histofix 4% and stained with 50 µg mL$^{-1}$ Concanavalin A conjugated with Alexa Fluor™ 647 (ConA-AF647; Thermo Fisher Scientific) at 37°C for 30 min to visualize external *Candida* cells. Coverslips were mounted with ProLong™ Gold Antifade Mountant with DAPI and fluorescence images were recorded using a Zeiss AXIO Observer.Z1 (Carl Zeiss Microscopy). Stationary phase cells expressing yEGFP and mCherry under the control of the *TEF1* promotor were diluted 1:20 into fresh YPD medium and incubated at 37°C for 2 h and 180 rpm. Washed and fixed cells were imaged on glass slides using a Zeiss AXIO Observer.Z1 (Carl Zeiss Microscopy). Yeast cells of different strain backgrounds were imaged with the same exposure time and fluorescence channel settings, and image processing was conducted with the same parameters.

### Statistics

Data are reported as scatterplot, line charts, or bar charts, each showing mean + standard deviation (SD). Presented results are from at least three independent biological replicates (growth assays), four independent biological replicates (flow cytometry analysis), and two independent biological replicates (qRT-PCR analysis). Macrophage survival experiments were done with immune cells originating from four independent blood donors per day, on at least two independent days. Data were analyzed using GraphPad Prism 5 (GraphPad Software, San Diego, USA). For statistical analysis of matched observations (macrophage experiments), a repeated measures ANOVA, and for non-matched observations (GFP fluorescence intensity experiments), a one-way ANOVA was performed. In both cases a Bonferroni's multiple comparison test was included. Statistically significant results are marked with asterisks. (*$P \leq 0.05$, **$P \leq 0.01$, ***$P \leq 0.001$, ****$P \leq 0.0001$).

### SUMMARY

Taken together, we have constructed plasmids for fluorescence reporter-based analysis that integrate into the *TRP1* locus of *C. glabrata*. We show that fluorescence levels depend on the strength of the promotor and promotor-specific induction conditions. Moreover, we used the overexpression system for heterologous expression of the well-characterized model antigen OVA. This provides a basis for future measurements of specific immune responses of T cells against *C. glabrata*. Finally, we showed that the *TRP1* locus is a suitable locus to (re-)integrate genes of interest, either with their native DNA sequence, with specific sequence variations or with alternative promotors, to investigate the role and function of these genes for fungal (patho)biology. The set of plasmids presented here expands the genetic toolbox available for use with *C. glabrata*.

### SUPPLEMENTARY DATA

Supplementary data are available at *FEMSYR* online.

### REFERENCES

Bolotin-Fukuhara M, Fairhead C. *Candida glabrata*: a deadly companion? *Yeast* 2014;**31**:279–88.

Brand A, MacCallum DM, Brown AJ *et al*. Ectopic expression of URA3 can influence the virulence phenotypes and proteome of *Candida albicans* but can be overcome by targeted reintegration of URA3 at the RPS10 locus. *Eukaryot Cell* 2004;**3**:900–9.

Branlant G, Branlant C. Nucleotide sequence of the *Escherichia coli* gap gene. Different evolutionary behavior of the NAD+-binding domain and of the catalytic domain of D-glyceraldehyde-3-phosphate dehydrogenase. *Eur J Biochem* 1985;**150**:61–66.

Brunke S, Quintin J, Kasper L *et al*. Of mice, flies–and men? Comparing fungal infection models for large-scale screening efforts. *Dis Model Mech* 2015;**8**:473–86.

Chapman-Smith A, Cronan JE, Jr. Molecular biology of biotin attachment to proteins. *J Nutr* 1999;**129**:477S–84S.

Citiulo F, Jacobsen ID, Miramón P *et al*. *Candida albicans* scavenges host zinc via Pra1 during endothelial invasion. *PLoS Pathog* 2012;**8**:e1002777.

Cormack BP, Bertram G, Egerton M *et al*. Yeast-enhanced green fluorescent protein (yEGFP): a reporter of gene expression in *Candida albicans*. *Microbiology* 1997;**143(Pt 2)**:303–11.

Davis DA, Bruno VM, Loza L *et al*. *Candida albicans* Mds3p, a conserved regulator of pH responses and virulence identified through insertional mutagenesis. *Genetics* 2002;**162**:1573–81.

Diekema D, Arbefeville S, Boyken L *et al*. The changing epidemiology of healthcare-associated candidemia over three decades. *Diagn Microbiol Infect Dis* 2012;**73**:45–48.

Falkow S. Molecular Koch's postulates applied to microbial pathogenicity. *Rev Infect Dis* 1988;**10 Suppl 2**:S274–276.

Frieman MB, McCaffery JM, Cormack BP. Modular domain structure in the *Candida glabrata* adhesin Epa1p, a beta1,6 glucan-cross-linked cell wall protein. *Mol Microbiol* 2002;**46**:479–92.

Gabaldón T, Carrete L. The birth of a deadly yeast: tracing the evolutionary emergence of virulence traits in *Candida glabrata*. *FEMS Yeast Res* 2016;**16**: fov110.

Galocha M, Pais P, Cavalheiro M *et al*. Divergent Approaches to Virulence in *C. albicans* and *C. glabrata*: Two Sides of the Same Coin. *Int J Mol Sci* 2019;**20**.

Gartenberg MR, Smith JS. The Nuts and Bolts of Transcriptionally Silent Chromatin in *Saccharomyces cerevisiae*. *Genetics* 2016;**203**:1563–99.

Gerami-Nejad M, Zacchi LF, McClellan M *et al*. Shuttle vectors for facile gap repair cloning and integration into a neutral locus in *Candida albicans*. *Microbiology* 2013;**159**:565–79.

Ghosh S, Navarathna DH, Roberts DD *et al*. Arginine-induced germ tube formation in *Candida albicans* is essential for

escape from murine macrophage line RAW 264.7. *Infect Immun* 2009;**77**:1596–605.

Gola S, Martin R, Walther A *et al*. New modules for PCR-based gene targeting in *Candida albicans*: rapid and efficient gene targeting using 100 bp of flanking homology region. *Yeast* 2003;**20**:1339–47.

Harms JS, Khan M, Hall C *et al*. Brucella Peptide Cross-Reactive Major Histocompatibility Complex Class I Presentation Activates SIINFEKL-Specific T Cell Receptor-Expressing T Cells. *Infect Immun* 2018;**86**:e00281–18.

Hosogaya N, Miyazaki T, Nagi M *et al*. The heme-binding protein Dap1 links iron homeostasis to azole resistance via the P450 protein Erg11 in *Candida glabrata*. *FEMS Yeast Res* 2013;**13**: 411–21.

Hünniger K, Lehnert T, Bieber K *et al*. A virtual infection model quantifies innate effector mechanisms and *Candida albicans* immune escape in human blood. *PLoS Comput Biol* 2014;**10**:e1003479.

Ishizuka J, Grebe K, Shenderov E *et al*. Quantitating T cell cross-reactivity for unrelated peptide antigens. *J Immunol* 2009;**183**:4337–45.

Ito K, Matsudomi N. Structural characteristics of hen egg ovalbumin expressed in yeast *Pichia pastoris*. *Biosci Biotechnol Biochem* 2005;**69**:755–61.

Jacobsen ID, Brunke S, Seider K *et al*. *Candida glabrata* persistence in mice does not depend on host immunosuppression and is unaffected by fungal amino acid auxotrophy. *Infect Immun* 2010;**78**:1066–77.

Janbon G, Quintin J, Lanternier F *et al*. Studying fungal pathogens of humans and fungal infections: fungal diversity and diversity of approaches. *Genes Immun* 2019;**20**:403–14.

Kasper L, Konig A, Koenig PA *et al*. The fungal peptide toxin Candidalysin activates the NLRP3 inflammasome and causes cytolysis in mononuclear phagocytes. *Nat Commun* 2018;**9**:4260.

Kitada K, Yamaguchi E, Arisawa M. Isolation of a *Candida glabrata* centromere and its use in construction of plasmid vectors. *Gene* 1996;**175**:105–8.

Knowles JR. The mechanism of biotin-dependent enzymes. *Annu Rev Biochem* 1989;**58**:195–221.

Krummey SM, Floyd TL, Liu D *et al*. *Candida*-elicited murine Th17 cells express high Ctla-4 compared with Th1 cells and are resistant to costimulation blockade. *J Immunol* 2014;**192**:2495–504.

Kurtzman CP, Robnett CJ. Phylogenetic relationships among yeasts of the 'Saccharomyces complex' determined from multigene sequence analyses. *FEMS Yeast Res* 2003;**3**:417–32.

Lane MD, Rominger KL, Young DL *et al*. The Enzymatic Synthesis of Holotranscarboxylase from Apotranscarboxylase and (+)-Biotin. Ii. Investigation of the Reaction Mechanism. *J Biol Chem* 1964;**239**:2865–71.

Lüttich A, Brunke S, Hube B. Isolation and amplification of fungal RNA for microarray analysis from host samples. *Methods Mol Biol* 2012;**845**:411–21.

Millon L, Manteaux A, Reboux G *et al*. Fluconazole-resistant recurrent oral candidiasis in human immunodeficiency virus-positive patients: persistence of *Candida albicans* strains with the same genotype. *J Clin Microbiol* 1994;**32**: 1115–8.

Miramón P, Dunker C, Windecker H *et al*. Cellular responses of *Candida albicans* to phagocytosis and the extracellular activities of neutrophils are critical to counteract carbohydrate starvation, oxidative and nitrosative stress. *PLoS One* 2012;**7**:e52850.

Miyazaki T, Izumikawa K, Yamauchi S *et al*. The glycosylphosphatidylinositol-linked aspartyl protease Yps1 is transcriptionally regulated by the calcineurin-Crz1 and Slt2 MAPK pathways in *Candida glabrata*. *FEMS Yeast Res* 2011;**11**:449–56.

Morschhäuser J, Michel S, Hacker J. Expression of a chromosomally integrated, single-copy GFP gene in *Candida albicans*, and its use as a reporter of gene regulation. *Mol Gen Genet* 1998;**257** 412–20.

Murad AM, Lee PR, Broadbent ID *et al*. CIp10, an efficient and convenient integrating vector for *Candida albicans*. *Yeast* 2000;**16**:325–7.

Navarathna DH, Das A, Morschhauser J *et al*. Dur3 is the major urea transporter in *Candida albicans* and is co-regulated with the urea amidolyase Dur1,2. *Microbiology* 2011;**157**:270–9.

Navarathna DH, Lionakis MS, Lizak MJ *et al*. Urea amidolyase (*DUR1,2*) contributes to virulence and kidney pathogenesis of *Candida albicans*. *PLoS One* 2012;**7**:e48475.

Nevitt T, Thiele DJ. Host iron withholding demands siderophore utilization for *Candida glabrata* to survive macrophage killing. *PLoS Pathog* 2011;**7**:e1001322.

Noble JA, Tsai HF, Suffis SD *et al*. STB5 is a negative regulator of azole resistance in *Candida glabrata*. *Antimicrob Agents Chemother* 2013;**57**:959–67.

Norrander J, Kempe T, Messing J. Construction of improved M13 vectors using oligodeoxynucleotide-directed mutagenesis. *Gene* 1983;**26**:101–6.

Pfaffl MW. A new mathematical model for relative quantification in real-time RT-PCR. *Nucleic Acids Res* 2001;**29**:e45.

Pla J, Gil C, Monteoliva L *et al*. Understanding *Candida albicans* at the molecular level. *Yeast* 1996;**12**:1677–702.

Rando OJ, Winston F. Chromatin and transcription in yeast. *Genetics* 2012;**190**:351–87.

Roon RJ, Levenberg B. Urea amidolyase. I. Properties of the enzyme from *Candida utilis*. *J Biol Chem* 1972;**247**:4107–13.

Samols D, Thornton CG, Murtif VL *et al*. Evolutionary conservation among biotin enzymes. *J Biol Chem* 1988;**263**:6461–4.

Sanglard D, Ischer F, Monod M *et al*. Susceptibilities of *Candida albicans* multidrug transporter mutants to various antifungal agents and other metabolic inhibitors. *Antimicrob Agents Chemother* 1996;**40**:2300–5.

Schwarzmüller T, Ma B, Hiller E *et al*. Systematic phenotyping of a large-scale *Candida glabrata* deletion collection reveals novel antifungal tolerance genes. *PLoS Pathog* 2014;**10**:e1004211.

Seider K, Gerwien F, Kasper L *et al*. Immune evasion, stress resistance, and efficient nutrient acquisition are crucial for intracellular survival of *Candida glabrata* within macrophages. *Eukaryot Cell* 2014;**13**:170–83.

Sprenger M, Hartung TS, Allert S *et al*. Fungal biotin homeostasis is essential for immune evasion after macrophage phagocytosis and virulence. *Cell Microbiol* 2020.

Staab JF, Bahn YS, Sundstrom P. Integrative, multifunctional plasmids for hypha-specific or constitutive expression of green fluorescent protein in *Candida albicans*. *Microbiology* 2003;**149**:2977–86.

Sternicki LM, Wegener KL, Bruning JB *et al*. Mechanisms Governing Precise Protein Biotinylation. *Trends Biochem Sci* 2017;**42**:383–94.

Tong L. Structure and function of biotin-dependent carboxylases. *Cell Mol Life Sci* 2013;**70**:863–91.

Ueno K, Matsumoto Y, Uno J *et al*. Intestinal resident yeast *Candida glabrata* requires Cyb2p-mediated lactate assimilation to adapt in mouse intestine. *PLoS One* 2011;**6**:e24759.

Vandeputte P, Ischer F, Sanglard D *et al.* In vivo systematic analysis of *Candida albicans* Zn2-Cys6 transcription factors mutants for mice organ colonization. *PLoS One* 2011;**6**: e26962.

Walther A, Wendland J. An improved transformation protocol for the human fungal pathogen *Candida albicans*. *Curr Genet* 2003;**42**:339–43.

Wilson RB, Davis D, Mitchell AP. Rapid hypothesis testing with *Candida albicans* through gene disruption with short homology regions. *J Bacteriol* 1999;**181**:1868–74.

Xu QR, Yan L, Lv QZ *et al.* Molecular genetic techniques for gene manipulation in *Candida albicans*. *Virulence* 2014;**5**:507–20.

Yánez-Carrillo P, Orta-Zavalza E, Gutierrez-Escobedo G *et al.* Expression vectors for C-terminal fusions with fluorescent proteins and epitope tags in *Candida glabrata*. *Fungal Genet Biol* 2015;**80**:43–52.

Zempleni J, Wijeratne SS, Hassan YI. Biotin. *Biofactors* 2009;**35**:36–46.

Zordan RE, Ren Y, Pan SJ *et al.* Expression plasmids for use in *Candida glabrata*. *G3 (Bethesda)* 2013;**3**:1675–86.